Performance Analysis of RIS-Assisted Bi-Directional Full-Duplex Systems Under Hardware Impairments and Nakagami-m Fading Channels

Rajesh Ramanathan, and Bagubali Annasamy

Original scientific article

***Abstract*—This paper investigates the performance of reflective intelligent surface (RIS)-assisted bi-directional full-duplex (FD) systems considering hardware impairments (HIs), and self-interference (SI) under Nakagami-m fading. Unlike previous research that assumes ideal hardware or Rayleigh fading, this work derives closed-form expressions for outage probability, asymptotic diversity, throughput, and energy efficiency. The analysis employs a novel Gamma approximation, based on moment-matching and a first-order Laguerre series expansion, to accurately model Nakagami-m product channels. The derived formulations allow efficient performance comparisons, including RIS-assisted half-duplex (HD) systems with and without hardware impairments. Numerical results reveal that using HIs/SI results in error floors. Increasing the number of reflective elements N, reduces the outage probability and enhances throughput and energy efficiency. The Monte Carlo simulations validate the analytical findings. Therefore, the proposed framework provides valuable design insights into the trade-offs among transceiver non-idealities, RIS size, and overall system robustness, serving as a critical reference for designing energy-efficient, hardware-aware RIS-assisted FD communication architectures in future wireless networks.**

***Index Terms*—Bi-directional, full-duplex, half-duplex, hardware impairments, reflective intelligent surface.**

I. Introduction

FIFTH-generation (5G) networks support diverse communication paradigms, including massive machine-type communication (mMTC), ultra-reliable low-latency communication (URLLC), and enhanced mobile broadband communication (eMBB).

Current 6G research emphasizes improvements in spectral efficiency and overall system performance. For instance, [3] studies conventional (C-RIS) and simultaneously transmitting and reflecting intelligent surfaces (STAR-RIS) in in-band FD systems to improve spectral efficiency and reduce SI by optimizing the number of C-RIS elements. [4] leverages STAR-RIS to enhance cell-edge user communication in FD non-orthogonal multiple access (NOMA) networks, thereby maximizing ergodic sum rate. [5] proposes an architecture for improved spectral efficiency via simultaneous full-spectrum uplink and downlink communication, optimizing beamforming and addressing SI cancellation. It also discusses transmitter-to-receiver interference in FD massive MIMO systems, outlining challenges, applications, and future research. [6] introduces a metasurface-based reconfigurable antenna architecture to enhance wireless communication through advanced analog signal processing. In [7], authors propose a STAR-assisted FD massive MIMO two-way network to improve coverage in weak-signal areas, optimizing the passive beamforming matrix to maximize spectral efficiency even with correlated channels and imperfect channel state information. Simulations demonstrate its superiority over half-duplex and conventional RIS-assisted systems. Finally, [8] examines the potential and challenges of the terahertz (THz) frequency band for future wireless communication to meet throughput demands, emphasizing spectrum expansion and discussing implications for mobile network simulations and Beyond-5G architectures. RIS-assisted NOMA systems' physical-layer security (PLS) is studied, using joint beamforming/power allocation to enhance PLS against internal/external threats. Noise beamforming reduces external eavesdropping. Simulations show more RIS elements improve secrecy more than transmit antennas [9].

Device-to-device (D2D) relaying challenges are reviewed, focusing on resource/interference management, assessing research limits and open questions [10]. Building upon these system modeling advancements, FD (FD) communication emerges as a critical enabler offering superior spectral efficiency and reduced latency. However, SI and cross-link interference in multi-cell deployments pose significant challenges to widespread FD adoption. Combining FD with emerging 6G technologies such as RIS and non-terrestrial networks (NTNs) creates a unified platform for integrated communication, sensing, and backhaul applications [11]. Therefore, the integration of RIS with FD technology is increasingly recognized as a pivotal approach for meeting the advanced demands of 6G wireless networks, enabling adaptable and efficient solutions.

RIS-assisted FD systems are garnering considerable research attention as a promising solution to meet the growing need for ultra-reliable and spectrally efficient wireless communication in 6G networks [12]. Existing research on the RIS-

Manuscript received December 11, 2025; revised January 8, 2026. Date of publication March 30, 2026. Date of current version March 30, 2026. The associate editor prof. Dragana Krstić has been coordinating the review of this manuscript and approved it for publication.

Authors are with the School of Electronics Engineering, Vellore Institute of Technology, Vellore, India (e-mails: rajesh@vit.ac.in, bagubali@vit.ac.in).

Digital Object Identifier (DOI): 10.24138/jcomss-2025-0261

aided FD systems with HIs often employs simplified one-way models or considers specific fading conditions (e.g., Rayleigh fading or correlated Nakagami-m fading without bi-directional HIs/SI). This paper addresses this gap by presenting a robust analytical framework to evaluate the performance of RIS-assisted bi-directional FD systems, accounting for HIs, SI, and Nakagami-m fading channels.

The key contributions of this paper are outlined below:

- In contrast to Rayleigh models, obtaining closed-form PDF/CDF expressions for products of Nakagami-m random variables presents a considerable challenge. To overcome this difficulty, we employ a moment-matching technique in conjunction with a first-order Laguerre series expansion to approximate the distribution. This method provides a more rigorous mathematical framework compared to prior investigations based on Rayleigh distributions.
- The framework presents a significant advancement over previous studies by offering closed-form expressions for all four key performance indicators in the specified configuration. This addresses a notable gap in the existing literature pertaining to rigorous energy efficiency analysis and asymptotic outage behavior.
- The analysis reveals SNR error floors attributable to hardware limitations and persistent SI. Moreover, the findings suggest that augmenting the number of reflecting elements N may reduce energy efficiency at higher SNRs, despite improved reliability. This represents a crucial design factor for implementations subject to hardware constraints.

The following sections of this paper are structured as follows: Section II presents the related works, Section III presents the system and channel models. Section IV presents the derivation of performance metrics, addressing outage probability, asymptotic outage probability, throughput, and energy efficiency. Section V provides numerical results accompanied by comprehensive discussion. Finally, section VI concludes with a summary of key insights.

II. Related Works

Research on the RIS systems has predominantly focused on the one-way transmission, often assuming ideal transceiver hardware [13]–[15]. However, practical transceivers are subject to impairments, including phase noise and amplifier nonlinearities, which can diminish RIS performance. Therefore, substantial research efforts have been dedicated to the evaluating RIS-enabled wireless systems, with particular emphasis on the effects of HIs in various fading channel environments. In [16], the authors examined a hybrid RIS-relay-assisted system, with an emphasis on the throughput and probability of outage performance in the presence of HIs. [17] analyzed the rate-energy trade-off in a simultaneous wireless power and information transfer RIS-enabled wireless networks, accounting for HIs. Additionally, heterogeneous networks supported by RIS (HetNets) [18] and satellite unmanned aerial vehicle (UAV)-terrestrial networks [19] were evaluated by considering the effect of HIs. In [20], massive MIMO systems assisted by RIS with HIs were analyzed using statistical channel state information (CSI). Reference [21] analyzed the performance metrics of RIS-enabled wireless systems in one way, focusing on the coverage probability and capacity, along with the energy and spectral efficiencies [22]. The expansion of this analysis to include systems featuring multiple inputs and a single output has been previously explored in [23]. Recently, analytical expressions were derived to enhance the spectral efficiency of a cell-free massive multiple input and multiple output (MIMO) system aided by an RIS with the impact of HIs in [24]. Upper limits for the ergodic sum-rate were analytically derived in [25] for both perfect and imperfect successive interference cancellation (SIC) decoding in NOMA systems using RIS. Furthermore, the advantages of incorporating relay and RIS technologies into wireless communication systems have been thoroughly investigated. Coverage analysis of this combined architecture is presented in [26], whereas power consumption and energy efficiency aspects are detailed in [27]. Therefore, it is essential to emphasize that the studies cited primarily addressed one-way transmission scenarios influenced by HIs.

Recently, RIS-assisted bi-directional communications have attracted considerable attention and have been extensively studied in the literature across various fading channels. The research cited in [28] explores bi-directional communication systems enhanced by an RIS, concentrating on the outage probability in one direction, spectral efficiency, and the effects of Rayleigh fading channel environment. The study presented in [29] explored a method for optimizing the base station's precoding matrix and RIS reflection coefficients to maximize the minimum weighted rate for users in multi-user, FD bi-directional systems that operate over Rician fading channels. In [30], a design was proposed that simultaneously optimizes the beamforming matrix and the RIS phase shifts for bi-directional communications enabled by RIS over channels that experience both Rayleigh and Rician fading. Reference [31] investigates the probability of outage and ergodic capacity of RIS-assisted bi-directional NOMA networks, specifically within the framework of Rayleigh fading. The study in [32] evaluated the performance of RIS-enabled bi-directional FD communications in the context of Rayleigh fading channels. Reference [33] investigated the sum-rate maximization problem of a RIS-assisted bidirectional system in a Rayleigh fading environment. In [34], RIS-aided device-to-device FD systems were analyzed, with a focus on key performance indicators such as the outage probability, ergodic capacity, throughput, and energy efficiency. In [35], a phase optimization method was proposed to achieve the maximum sum rate in RIS-assisted bi-directional relay networks. In [36] a bi-directional FD wireless system employing multiple RIS was investigated, with a focus on the joint optimization of RIS dimensions and positioning. In [37], RIS-assisted bi-directional FD communications were investigated, with key performance metrics such as the outage probability, considering non-reciprocal channels. However, recent studies [38], [39] have highlighted the potential of integrating RIS in bi-directional FD systems to improve wireless communication, particularly in light of HIs. References [40] specifically investigated the RIS-aided system performance in the presence of HIs, providing crucial insights

into practical limitations. In [41], [42], the authors explored FD RIS system with Rayleigh fading and SI, deriving expressions for outage probability, ergodic capacity, and error rate, and examines the impact of metasurface configuration and system parameters on performance. Additionally, [43] investigated the RIS-supported bi-directional FD systems, noting that SI and hardware limitations caused substantial performance deterioration, leading to capacity saturation and increased error rates. Reference [44] investigates UAV-assisted communication, addressing energy constraints and security risks by using simultaneous wireless information and power transfer (SWIPT) with cooperative jamming. Reference [45] explores secure communication via simultaneously transmitting and reflecting reconfigurable intelligent surfaces (STAR-RIS), using deep reinforcement learning to optimize signal transmission and enhance security against eavesdropping. More recently, [46] introduced a novel approach for joint communication and sensing, integrating communication and radar functionalities into a unified device by combining an RIS with a FD MIMO node optimized for efficient SI management. Finally, [47] presents a study of an RIS in a FD (FD) communication network, deriving closed-form expressions for signal power distribution in correlated Nakagami-m channel fading, and demonstrating that FD outperforms half-duplex (HD) communication below a defined threshold.

III. System Model

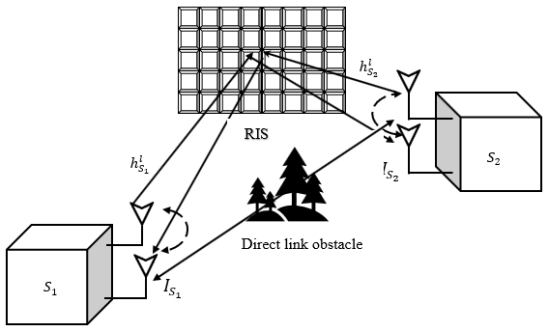

Fig. 1. RIS-FD-HIs System model.

Consider the RIS-assisted bi-directional FD system model shown in Fig.1 consisting of two source nodes, S_1 and S_2 communicating through RIS. An RIS consists of N reflective metasurface elements capable of adjusting the phases of incident signals. Operating in FD mode, both source nodes S_1 and S_2 simultaneously transmit and receive signals, which leads to SI. Moreover, the source nodes are assumed to not be directly connected because of natural or man-made obstacles. The channel fading coefficient between the source nodes $S_n(n \in \{1,2\})$ and the RIS is denoted as $h^l_{S_n} = \left[h^1_{S_n}, h^2_{S_n}, \ldots, h^N_{S_n}\right]^T$, $n \in \{1,2\}$. Where T signifies the channel vector transpose. Each element of the complex channel fading coefficient $h^l_{S_n}$ is defined as $h^l_{S_n} = \left|h^l_{S_n}\right| e^{j\theta}$, with $l = 1,2,\ldots,N$ and $n \in \{1,2\}$. The channel fading follows a Nakagami-m distribution characterized by a shape parameter m, scale parameter Ω, and phase θ which is uniformly distributed between 0 and 2π. The Nakagami-m channel fading distribution offers a comprehensive framework for modeling the fading characteristics of wireless channels. Unlike Rayleigh fading, this distribution uses the m parameter to represent different fading conditions. By considering the impact of HIs from both source nodes $S_n(n \in \{1,2\})$, the signal received at the l^{th} element of RIS [48] can be expressed as

$$y_{RIS} = \sqrt{P_s}\left[h^l_{S_1}(x_1 + \eta^t_{S_1}) + h^l_{S_2}(x_2 + \eta^t_{S_2})\right] e^{j\phi^l} \quad (1)$$

where ϕ^l represents the adjustable phase shift of the l^{th} element in the RIS, and x_1 and x_2 be the transmitted data symbols. P_s denotes the transmit power at each source node $S_n(n \in \{1,2\})$, and $h^l_{S_n}$, $l = 1,2,...N$, $n \in \{1,2\}$, denotes the complex channel fading coefficient between the source nodes $S_n(n \in \{1,2\})$, and RIS paths. The term $\eta^t_{S_n}$, $n \in \{1,2\}$ represents the transmit HIs distortion, modeled as $\eta^t_{S_n} \sim \mathcal{CN}(0,(k^t_{S_n})^2 P_s)$, and $k^t_{S_n}$, $n \in \{1,2\}$ denotes the transmit error vector magnitude (EVM). similarly, $\eta^r_{S_n}$, at $n \in \{1,2\}$ is the receive HIs distortion modeled as $\eta^r_{S_n} \sim \mathcal{CN}\left[0, \sum_{l=1}^N \left|h^l_{S_1} h^l_{S_2} e^{j\phi^l}\right|^2 (k^r_{S_n})^2 P_s\right]$, and $k^r_{S_n}$, $n = 1,2$ is the receive EVM respectively [49]. Assuming perfect CSI, the RIS optimally selects the continuous phase shift ϕ^l for each element N. This enables dynamic phase control, thereby maximizing the strength of the received signal [40]. However, in practice, CSI imperfections—due to estimation errors, feedback latency, and hardware limitations—cause phase misalignment and reduce beamforming efficiency. The hardware constraints in practical systems limit phase adjustments to a discrete set as $\nabla = \{0, 2\pi/Q, 4\pi/Q, \ldots, 2\pi(Q-1)/Q\}$, where the phase resolution $Q = 2^b$ depends on the number of control bits b. With sufficient phase resolution ($Q >> 1$) and complete CSI, approximating the ideal optimal phase shift becomes feasible.

The received signal, y_{RIS}, is transmitted back to source nodes S_1 and S_2 via the reciprocal channel $h^l_{S_n,m}$, $n \in \{1,2\}$. Therefore, at the source nodes, $S_n(n \in \{1,2\})$, the received signal can be written as

$$y_{S_n} = \sum_{l=1}^{N} h^l_{S_n} y_{RIS} + \eta^r_{S_n} + I_{S_n} + z_{S_n} \quad (2)$$

By substituting (1) in (2), the source node S_1 signal received is written as

$$\begin{aligned} y_{S_1} = & \underbrace{\sqrt{P_s}\sum_{l=1}^{N}\left|h^l_{S_1}\right|^2 (x_1 + \eta^t_{S_1}) e^{j\phi^l}}_{\text{Self-Information Signal and associated HIs}} \\ & + \underbrace{\sqrt{P_s}\sum_{l=1}^{N}\left|h^l_{S_1}\right|\left|h^l_{S_2}\right| (x_2 + \eta^t_{S_2}) e^{j\phi^l}}_{\text{Desired Signal and associated HIs}} \\ & + \underbrace{\eta^r_{S_1}}_{\text{Source node } S_1 \text{ HIs}} + \underbrace{I_{S_1}}_{\text{Self interference}} + \underbrace{z_{S_1}}_{\text{Noise}} \end{aligned} \quad (3)$$

In (3), the first term represents the self-information signal consisting of its own transmit symbol x_1 transmitted by source node S_1 and the associated HIs. The second term corresponds to the desired signal and its associated HIs. The third term $\eta^r_{S_1}$, represents the HIs induced by S_1. The fourth term I_{S_1} represents the SI at the source nodes S_1 formulated as $I_{S_1} \sim \mathcal{CN}(0, \ell^2_{S_1} P_s)$, and the fifth term represents the additive white Gaussian noise (AWGN), formulated as $z_{S_1} \sim \mathcal{CN}(0, \sigma^2_{S_1})$, respectively.

Similarly, source node S_2 received signal can be written as

$$\begin{aligned} y_{S_2} &= \sqrt{P_s} \sum_{l=1}^{N} \left|h^l_{S_2}\right|^2 (x_2 + \eta^t_{S_2}) e^{j\phi^l} \\ &+ \sqrt{P_s} \sum_{l=1}^{N} \left|h^l_{S_1}\right| \left|h^l_{S_2}\right| (x_1 + \eta^t_{S_1}) e^{j\phi^l} \\ &+ \eta^r_{S_2} + I_{S_2} + z_{S_2} \end{aligned} \tag{4}$$

After subtracting the self information signal from (3) and (4), and aggregating the distortion caused by the source nodes HIs, the received source node $S_n (n \in \{1, 2\})$ signals can be expressed as

$$y_{S_n} = \sqrt{P_s} \sum_{l=1}^{N} \left|h^l_{S_1}\right| \left|h^l_{S_2}\right| (x_n + \eta_{S_1 S_2}) \, e^{j\phi^l} + I_{S_n} + z_{S_n} \tag{5}$$

where $\eta_{S_1 S_2} \sim \mathcal{CN}\left(0, \sum_{l=1}^{N} \left|h^l_{S_1} h^l_{S_2}\right|^2 k^2_{S_1 S_2} P_s\right)$ be the aggregate distortion caused at S_n, $n = 1, 2$ nodes, $k^2_{S_1 S_2} = (k^t_{S_1})^2 + (k^r_{S_2})^2$, $k^2_{S_2 S_1} = (k^t_{S_2})^2 + (k^r_{S_1})^2$, is the EVM at S_n, $n = 1, 2$, $h^l_{S_1} = \zeta^l_{S_1} e^{-j\psi^l_{S_1}}$ and $h^l_{S_2} = \zeta^l_{S_2} e^{-j\psi^l_{S_2}}$. $\zeta^l_{S_n}$ are the magnitudes and $e^{-j\psi^l_{S_n}}$, $n \in \{1, 2\}$ are the phases of $h^l_{S_2}$ and $h^l_{S_2}$ respectively.

By substituting for $h^l_{S_1}$ and $h^l_{S_2}$ in (5), at source nodes $S_n (n \in \{1, 2\})$, the received signal can be written as

$$\begin{aligned} y_{S_n} &= \sqrt{P_s} \sum_{l=1}^{N} \zeta^l_{S_1,m} \zeta^l_{S_2} e^{j\left(\phi^l - \psi^l_{S_1} - \psi^l_{S_2}\right)} (x_n + \eta_{S_1 S_2}) \\ &+ \; I_{S_n} + z_{S_n} \end{aligned} \tag{6}$$

Then, the SI cancellation at nodes S_1 and S_2 employs integrated antenna, analog, and digital methods [48], [50]. Antenna-based techniques, including polarization diversity and directional antennas, reduce SI by $40 - 60$ dB [50]. Optimized antenna design and signal processing enable analog and digital cancellation of $20 - 35$ dB and 20-40 dB, respectively [50]. Combining these approaches achieves an overall attenuation of $80 - 120$ dB, effectively suppressing SI to the noise floor [50]. The residual SI after digital cancellation, being post-quantization, is typically modeled as a Gaussian random variable, a characterization supported by measurements and modeling [43], [48], [50]. Following the implementation of all three cancellation techniques, the instantaneous signal-to-interference-plus-noise-and-distortion ratio (SINDR) at the source node $S_n (n \in \{1, 2\})$ is expressed for the proposed system as:

$$\gamma^{RIS-HIs}_{S_n} = \frac{\left|\sum_{l=1}^{N} \zeta^l_{S_1} \zeta^l_{S_2} e^{j\left(\phi^l - \psi^l_{S_1,m} - \psi^l_{S_2,m}\right)}\right|^2 P_s}{\left|\sum_{l=1}^{N} \zeta^l_{S_1} \zeta^l_{S_2}\right|^2 k^2_{S_1 S_2} P_s + \ell^2_{S_n} P_s + \sigma^2_{S_n}} \tag{7}$$

where $\gamma^{RIS-HIs}_{S_n}$ denotes the maximum instantaneous SINDR at the source node $S_n (n \in \{1, 2\})$ and $\ell^2_{S_n}$ denotes the self interference level at the source nodes S_n. The phases of RIS can be configured to maximize the SINR at the source nodes $S_n (n \in \{1, 2\})$ is given by $\phi^l = \psi^l_{S_1,m} + \psi^l_{S_2,m}, l = 1, 2, \ldots, N_m$.

Therefore, at the source nodes $S_n (n \in \{1, 2\})$, the instantaneous SINDR of the proposed system can be written as

$$\gamma^{RIS-HIs}_{S_n} = \frac{\left|\sum_{l=1}^{N} \zeta^l_{S_1} \zeta^l_{S_2}\right|^2 P_s}{\left|\sum_{l=1}^{N} \zeta^l_{S_1} \zeta^l_{S_2}\right|^2 k^2_{S_1 S_2} P_s + \ell^2_{S_n} P_s + \sigma^2_{S_n}} \tag{8}$$

A. Statistical Characteristics of Channel Model

Based on the realistic Nakagami-m fading model, we introduce key distributions of random variables (RVs) that will assist us in performing analytical derivations on the performance metrics.

$$Z = \sum_{l=1}^{N} \zeta^l_{S_1} \zeta^l_{S_2}, \quad n = 1, 2 \tag{9}$$

Let $\zeta^l_{S_n,m}$, for $l = 1, 2, \ldots, N$ and $n = 1, 2$, denote Nakagami-m distributed random variables characterized by the shape and scale parameters m_1, m_2, Ω_1, and Ω_2, respectively. Within the framework of Nakagami-m fading model, the random variable (RV) $Z_l = \zeta^l_{S_1} \zeta^l_{S_2,m}$ is critical in analyzing the performance characteristics of the proposed system. The variable Z_l represents the product of Nakagami-m random variables. Deriving a closed-form expression for the probability density function (PDF) and cumulative distribution function (CDF) presents significant analytical challenges, as discussed in [40]. Therefore, we utilize the moment matching approach to estimate the distribution of the random variable Z_l by employing a Gamma distribution for every value of N.

Theorem 1.

According to Gamma distribution, the CDF of the proposed RIS-assisted bi-directional FD system incorporating HIs and SI is expressed as

$$F_{\gamma_{S_n}}(x) \simeq \frac{1}{\Gamma(a+1)} \gamma\left(a + 1, \frac{1}{b} x\right) \tag{10}$$

where $\gamma(\cdot, \cdot)$ denotes the lower incomplete gamma function [51], defined as $\gamma(s, x) = \int_0^x t^{s-1} e^{-t} \, dt$, $x = \sqrt{\frac{\left(\ell^2_{S_n} P_s + \sigma^2_{S_n}\right) \gamma_{th}}{P_s \left(1 - k^2_{S_1 S_2} \gamma_{th}\right)}}$, and $\gamma_{th} = 2^{\Re} - 1$ is the SINDR threshold, with the data rate of $\Re$ in bits per channel use (BPCU).

Proof. Let $Z_l = \zeta^l_{S_1,m}\zeta^l_{S_2,m}$ represent a random variable that follows the Nakagami-m distribution, characterized by the shape and the scale parameters m_1, m_2, Ω_1 and Ω_2 respectively. By using [52], the PDF of Z_l is given by

$$f_{Z_l}(z) = \frac{4\left(\frac{m_1 m_2}{\Omega_1\Omega_2}\right) z^{m_1+m_2-1}}{\Gamma(m_1)\Gamma(m_1)} \times K_{m_1-m_2}\left(2z\sqrt{\frac{m_1 m_2}{\Omega_1\Omega_2}}\right) \tag{11}$$

where $K_v(.)$ refers to the v^{th} order modified Bessel function of the second kind as defined in [51]. Subsequently, the mean and variance of Z_l are given by

$$E[Z_l] = \left(\sqrt{\frac{\Omega_1\Omega_2}{m_1 m_2}}\right)\left(\frac{\Gamma(m_1+1/2)^2}{\Gamma(m_1)\Gamma(m_2)}\right) \tag{12}$$

and

$$Var[Z_l] = \Omega_1\Omega_2\left[1 - \frac{\Gamma(m_1+0.5)^2\Gamma(m_2+0.5)^2}{\Gamma(m_1)^2\Gamma(m_2)^2}\right] \tag{13}$$

where the Gamma function [51] is given by $\Gamma(.)$. The distribution of the RV $Z = \sum_{l=1}^{N_m} Z_l$ is is approximated by a Gamma distribution, derived from a first-order Laguerre series expansion [53], and the PDF can be expressed as

$$f_Z(z) = \frac{z^a e^{(-z/b)}}{\Gamma(a+1)b^{(a+1)}} \tag{14}$$

The Gamma distribution's shape parameter a and the scale parameter b, can be expressed in terms of $E(Z_l)$ and $Var(Z_l)$ as follows: $a = ((E(Z_l))^2/Var(Z_l)) - 1$, and $b = Var(Z_l)/E(Z_l)$. By substituting (12) and (13) in a and b, it can be written as

$$a = \frac{m_1 m_2 N\Gamma(m_1)^2\Gamma(m_2)^2}{m_1 m_2\Gamma(m_1)^2\Gamma(m_2)^2 - \Gamma(m_1+0.5)^2\Gamma(m_2+0.5)^2} - (N+1) \tag{15}$$

and

$$b = \frac{\Gamma(m_1)^2\Gamma(m_2)^2 m_1 m_2 - \Gamma(m_1+0.5)^2\Gamma(m_2+0.5)^2}{\sqrt{\frac{m_1}{\Omega_1}}\Gamma(m_1+0.5)\Gamma(m_1)\sqrt{\frac{m_2}{\Omega_2}}\Gamma(m_2+0.5)\Gamma(m_2)} \tag{16}$$

where $E(Z_l) = NE(Z_l)$ and $Var(Z_l) = NVar(Z_l)$.

The CDF of random variable Z [54] is defined as the integral

$$F_Z(z) = \int_0^z f_Z(t)\,dt \tag{17}$$

By substituting the approximate PDF derived from (14) in (17)

$$F_Z(z) \simeq \int_0^z \frac{1}{\Gamma(a+1)b^{a+1}} t^a e^{-t/b} dt \tag{18}$$

Let $u = t/b$, then $t = ub$, and $dt = bdu$. Upon substitution, the limits of integration transform such that $t = 0$ becomes $u = 0$, and $t = z$ becomes $u = z/b$ Consequently, the integral is now expressed as

$$F_Z(z) \simeq \frac{1}{\Gamma(a+1)} \int_0^{\frac{z}{b}} \frac{1}{b^{a+1}} (ub)^a e^{-u} b\ du \tag{19}$$

After simplifying the above equation

$$F_Z(z) \simeq \frac{1}{\Gamma(a+1)} \int_0^{\frac{z}{b}} u^a e^{-u}\ du \tag{20}$$

By applying the lower incomplete gamma function $\gamma(a+1,x) = \int_0^x t^a e^{-t} dt$ introduced earlier completes the proof of (10) and the accuracy of this method relies on the first term of the Laguerre series expansion, constituting a reasonable, though approximate, simplification.

IV. Performance Evaluation of RIS-Assisted Bi-directional Full Duplex system

In this section, we analyze the performance of the proposed RIS-assisted bi-directional FD communication system. This analysis considers the effect of HIs and SI under te Nakagami-m fading conditions.

A. Outage Probability

The outage performance of the proposed RIS-assisted bi-directional FD hardware impairments (RIS-FD-HIs) system is evaluated by analyzing the probability that the instantaneous SINDR $\gamma^{RIS-HIs}_{S_n}$ drops below a specified threshold γ_{th} [55]. The outage probability is then mathematically formulated as

$$P^{RIS-HIs}_{out} = \Pr(\gamma^{RIS-HIs}_{S_n} < \gamma_{th}), n = 1, 2 \tag{21}$$

Using (8), the outage probability is expressed as

$$\begin{aligned} P^{\text{RIS-HIs}}_{out} &= \Pr\left\{\left|\sum_{l=1}^{N} \zeta^l_{S_1}\zeta^l_{S_2}\right|^2 P_s\left(1 - k^2_{S_1S_2}\gamma_{th}\right) \right. \\ &\quad \left. < \left(\ell^2_{S_n} P_s + \sigma^2_{S_n}\right)\gamma_{th}\right\} \\ &= \Pr\left\{Z^2 < \frac{(\ell^2_{S_n} P_s + \sigma^2_{S_n})\gamma_{th}}{P_s\left(1 - k^2_{S_1S_2}\gamma_{th}\right)}\right\} \end{aligned} \tag{22}$$

The proposed RIS-FD-HIs system outage probability is then formulated as

$$P^{RIS-HIs}_{out} = F_Z\left(\sqrt{\frac{\left(\ell^2_{S_n} P_s + \sigma^2_{S_n}\right)\gamma_{th}}{P_s\left(1 - k^2_{S_1S_2}\gamma_{th}\right)}}\right) \tag{23}$$

A separate closed-form expression for the outage probability is not provided, as it can be directly obtained from the CDF in (10) by evaluating at the target SINDR threshold γ_{th}.

B. Asymptotic Outage Probability

This subsection presents a comprehensive derivation of the asymptotic outage probability, emphasizing the system's performance under conditions of high signal-to-noise ratio (SNR) [40]. Therefore, the asymptotic outage probability of the proposed system can be expressed as

$$P^{Asymp}_{out} = F^{\infty}_{\gamma}(\gamma_{th}) \tag{24}$$

Using $\gamma(\alpha, x) = \sum_{n_m=0}^{\infty} \frac{(-1)^{n_m} x^{\alpha+n_m}}{n_m!(\alpha+n_m)}$ from [40], [51], and by substituting $\alpha = a+1$ and $x = \frac{1}{b}\sqrt{\frac{\left(\ell_{S_n}^2 P_s + \sigma_{S_n}^2\right)\gamma_{th}}{P_s\left(1-k_{S_1S_2}^2\gamma_{th}\right)}}$ in (24), the asymptotic outage probability can be expressed as

$$F_{\gamma}^{\infty}(\gamma_{th}) = \sum_{n_m=0}^{\infty} \frac{(-1)^{n_m}\left(\frac{1}{b}\sqrt{\frac{\left(\ell_{S_n}^2 P_s + \sigma_{S_n}^2\right)\gamma_{th}}{P_s\left(1-k_{S_1S_2}^2\gamma_{th}\right)}}\right)^{a+1+n_m}}{n_m!(a+1+n_m)\Gamma(a+1)} \tag{25}$$

As the SNR values approaches to infinity in (25), the initial summation term, corresponding to $n_m = 0$, becomes the dominant factor. This is due to the higher-order power terms diminishing in significance relative to the lower-order terms [56]. Therefore, the asymptotic outage probability can be expressed as

$$P_{out}^{Asymp} = \frac{\left(\frac{\left(\ell_{S_n}^2 P_s + \sigma_{S_n}^2\right)\gamma_{th}}{P_s\left(1-k_{S_1S_2}^2\gamma_{th}\right)}\right)^{\left(\frac{a+1}{2}\right)}}{(a+1)b^{(a+1)}\Gamma(a+1)} \tag{26}$$

The asymptotic outage probability P_{out}^{Asymp} in the regime of high SNR can be expressed as $P_{out}^{Asymp} = (G_c\gamma)^{-G_d}$, where G_d represents the diversity order and asymptotic SNR (array) or diversity gain as G_c. Based on (26), the diversity order $G_d = (a+1)/2$ and G_c as $\frac{\left(\ell_{S_n}^2 P_s + \sigma_{S_n}^2\right)\gamma_{th}}{P_s\left(1-k_{S_1S_2}^2\gamma_{th}\right)(a+1)b^{(a+1)}\Gamma(a+1)}$. It is worth noting that G_c characterizes the horizontal shift of the outage curve at high SNR and does not represent any channel coding gain, as no channel coding scheme is employed in this study.

C. System Throughput

System throughput is a vital parameter for both analysis and optimization. It is defined as the average data rate successfully achieved across fading channels [58]. Mathematically, the throughput of the proposed system can be written as

$$\bar{\mathcal{T}}_{put}^{sys} = \mathcal{T}_{S_1S_2} + \mathcal{T}_{S_2S_1} \tag{27}$$

where $\mathcal{T}_{S_1S_2}$ is the throughput from source node S_1-to-source node S_2 and $\mathcal{T}_{S_2S_1}$ is the throughput from source node S_2-to-source node S_1. Since it is a symmetric system model assumption, the outage probability is same in both direction. Hence, this simplification makes the analysis more tractable. With this assumption, the throughput's $\mathcal{T}_{S_1S_2}$ and $\mathcal{T}_{S_2S_1}$ are equal. Therefore, the system throughput in terms of outage probability can be given as

$$\bar{\mathcal{T}}_{put}^{sys} = 2\Re(1 - P_{out}^{RIS-HIs}) \tag{28}$$

By substituting (10) in (28), the proposed system throughput is computed as

$$\bar{\mathcal{T}}_{put}^{sys} = 2\Re\left[\frac{\gamma\left(a+1, \frac{1}{b}\left(\sqrt{\frac{\left(\ell_{S_n}^2 P_s + \sigma_{S_n}^2\right)\gamma_{th}}{P_s\left(1-k_{S_1S_2}^2\gamma_{th}\right)}}\right)\right)}{\Gamma(a+1)}\right] \tag{29}$$

D. Energy Efficiency

In addition to outage probability and system throughput, energy efficiency is another critical performance indicator for evaluating the effectiveness of the proposed system [21]. The system's energy efficiency is defined as

$$\eta = \frac{B\bar{\mathcal{T}}_{put}^{sys}}{P_t} \tag{30}$$

where B denotes the bandwidth, $\bar{\mathcal{T}}_{put}^{sys}$ denotes the system throughput, and total power consumption $P_t = 2(P_{S_1} + N\bar{P}_l + \bar{P}_{S_1} + \bar{P}_{S_2})$ of proposed RIS-FD-HIs.

Therefore, by substituting (29) in (30), the energy efficiency is computed as

$$\eta = \frac{2\Re B}{P_t}\left[\frac{\gamma\left(a+1, \frac{1}{b}\left(\sqrt{\frac{\left(\ell_{S_n}^2 P_s + \sigma_{S_n}^2\right)\gamma_{th}}{P_s\left(1-k_{S_1S_2}^2\gamma_{th}\right)}}\right)\right)}{\Gamma(a+1)}\right] \tag{31}$$

where $\bar{P}_l$ signifies the power dissipation of the circuit, and $\bar{P}_{S_n}$, $n = 1, 2$ represents the source nodes power levels . Furthermore, as shown in (31), a linear relationship exists between power consumption and the number of reflective elements, N.

E. Impact of Imperfect CSI at RIS-FD

The perfect CSI at the RIS allows ideal phase alignment for performance analysis. However, CSI is imperfect in practice, leading to phase estimation errors and reduced effective channel gain [42]. Imperfect CSI mainly degrades the SINDR numerator in (8), while leaving the denominator largely unaffected. This leads to increased outage probability and reduced throughput, especially at moderate-to-high SNR where phase misalignment dominates. However, the SINDR's fundamental structure and analytical trends remain. Imperfect CSI mainly causes array gain loss, shifting outage curves upward without changing their asymptotic slope. Therefore, increasing RIS elements can compensate for CSI imperfections by improving signal power through spatial diversity. Even with long-term CSI or statistical CSI, the framework provides performance bounds. Future investigations will address imperfect CSI by employing phase error modeling or modified channel statistics.

V. Numerical Results and Discussion

In this section, we examine the performance of the proposed RIS-FD-HIs system. Monte Carlo simulations validate analytical results. Table I compares the proposed method with

TABLE I
COMPARISON OF PROPOSED METHOD WITH EXISTING RIS-ASSISTED FD/HD METHODS

Ref	*System Model*	*Channel Model*	*Impairments*		*Performance Metrics*			
			HIs	*SI*	*Outage Probability*	*Asymptotic Outage Probability*	*System Throughput*	*Energy Efficiency*
[33]	FD	Rayleigh	×	√	√	×	×	×
[38]	FD	Rayleigh	×	√	√	×	×	×
[57]	HD	Nakagami-m	√	×	√	√	×	×
[42]	FD	Corr. Rayleigh	√	√	√	×	×	×
[41]	HD	Rayleigh	√	×	√	×	×	×
[43]	FD	Rayleigh	×	√	√	×	×	×
[46]	FD	Rayleigh	√	√	√	×	×	×
[49]	FD	Rayleigh	√	√	√	×	×	×
Proposed	*FD*	*Nakagami-m*	√	√	√	√	√	√

TABLE II
LIST OF SIMULATION PARAMETERS

Symbol	*Parameters*	*Values*
S_n	Number of Source nodes	2
N	Number of reflective elements	$1-50$
$m_1 = m_2 = m$	Shape parameter	1, and 2
$\Omega_1 = \Omega_2 = \Omega$.	scale parameter	1
$\ell^2_{S_n}$	Self-interference level	$0-2$
$k^2_{S_1S_2}$	Hardware Impairments level	$0.01-0.03$
SNR	Signal to Noise Ratio	$-20dB-40$ dB
P_l	Circuit power dissipation of RIS element	6 dBm
$\sigma^2_{S_n}$.	Noise variance	1

existing methodologies under Nakagami-m fading, evaluating performance in terms of outage probability, throughput, and energy efficiency. The analysis considers key parameters such as the number of reflecting elements N, SI $\ell^2_{S_n}$, HIs $k^2_{S_1S_2}$, SNR, and data rate $\Re$. The proposed work offers a more comprehensive analysis by examining the influence of these various performance parameters. To the best of our knowledge, no prior research has investigated RIS-assisted bi-directional FD systems over Nakagami-m fading channels with respect to this range of performance parameters. The parameters employed for the performance analysis are detailed in Table II.

Fig. 2 presents the outage performance of the proposed RIS-assisted bi-directional FD communication system incorporating HIs under Nakagami-m fading environment. The evaluation is carried out at a data rate of $\Re = 4$ BPCU, $\Omega_1 = \Omega_2 = 1$, $m = 1$, $\ell^2_{S_n} = 0.1$, $N = 4, 8, 16$, and 32, and $k^2_{S_1S_2} = 0.01$. Based on (10), the analytical results indicate the performance degradation caused by the HIs and SI. Specifically, at $N = 4$ and 8 the impact of both HIs and SI yields a substantial degradation in performance, resulting in an error floor of SNR around $=$ 20dB. However, increasing $N \geq 16$ yields a substantial improvement in the outage probability below 10^{-4}, effectively mitigating the adverse effects of both HIs and SI, guiding minimum RIS sizing for reliability. Analytical results confirm HIs/SI-induced saturation. Quantitative analysis shows that $N \geq 16$ minimizes error floors, achieving a 10^{-4} outage at realistic SNR 20 dB, providing a design recommendation for RIS deployments. Furthermore, the asymptotic analysis

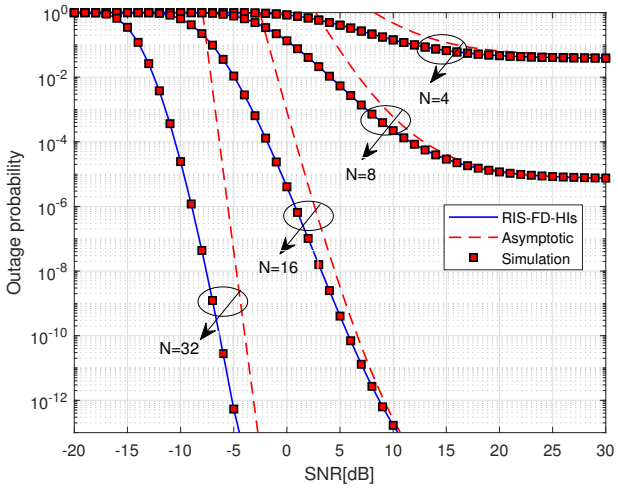

Fig. 2. Outage performance of the proposed RIS-FD-HIs versus SNR.

TABLE III
OUTAGE PERFORMANCE COMPARISON OF THE PROPOSED RIS-FD-HIS WITH THE BENCHMARK METHODS

SNR (dB)	*Reflective Elements N*	*Proposed RIS-FD-HIs*	*RIS-FD-IHIs*	*RIS-HD-HIs*	*RIS-HD-IHIs*
20	4	10^{-2} (error floor)	8×10^{-3}	10^{-4}	10^{-5}
20	8	5×10^{-3}	2×10^{-3}	10^{-5}	10^{-6}

derived from (26) closely approximates system performance at high signal-to-noise ratios (SNRs) by considering the dominant term and disregarding lower-order terms. Negative SNR values were included to assess system performance under low-SNR conditions, where HIs and SI are prominent. This range enables error floor identification and validation of asymptotic trends. Monte Carlo simulations further validate these analytical findings.

Fig. 3 presents a comparative analysis of the outage performance of the proposed RIS-assisted FD-HIs system in relation to RIS-FD-IHIs, RIS-HD-HIs, and RIS-HD-IHIs. The evaluation was performed with the following parameter configurations: $m = 2$, $\Omega_1 = \Omega_2 = 1$, $\Re = 4$, $k^2_{S_1S_2} = 0.01$, $\ell^2_{S_n} = 0.1$, and $N = 4$ and 8. Monte Carlo simulations thoroughly confirm the analytical findings. The numerical

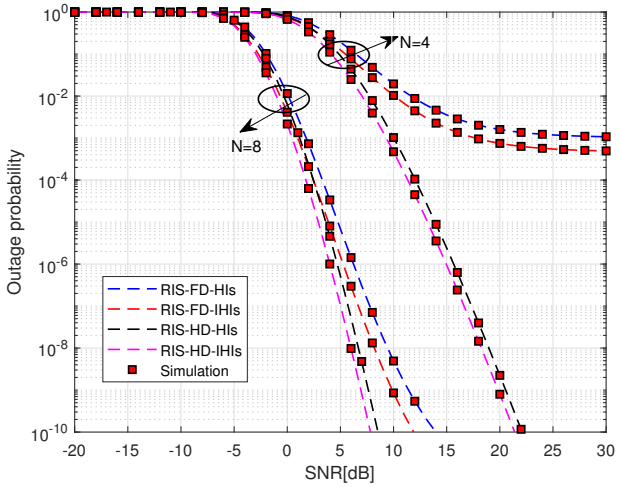

Fig. 3. Outage probability versus SNR of proposed RID-FD-HIs in comparison to RIS-FD-IHIs, RIS-HD-HIs, and RIS-HD-IHIs configurations at $N = 4$ and 8 reflective elements.

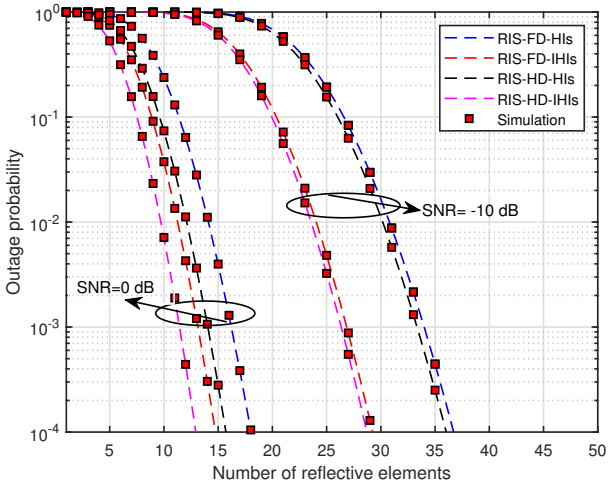

Fig. 4. Outage performance versus the number of reflective elements N.

results highlight the considerable impact of both HIs and SI on the system performance. For instance, with $N = 4$ the proposed RIS-FD-HIs system exhibits an error floor in outage probability around 25 dB SNR. Similarly, in the case of $N = 4$ with $l^2_{S_n} = 0$, the outage probability of RIS-FD-IHIs exhibits a saturation effect at a comparable SNR level, suggesting that SI significantly affects the performance. In contrast, with $N = 4$, the RIS-HD-HIs and RIS-HD-IHIs systems outage probability decreases rapidly with increasing SNR. This observation suggests that the impact of SI is more pronounced than that of HIs in these conditions. For the case of $N = 8$, the outage probabilities of all four systems (RIS-FD-HIs, RIS-FD-IHIs, RIS-HD-HIs, and RIS-HD-IHIs) decrease with increasing SNR within the range of 8 dB 15 dB, influenced by both HIs and SI. Therefore, augmenting N substantially mitigates the aggregate impact of HIs and SI. It can be observed from the outage comparative analysis Table III that in RIS-assisted FD systems, HIs and SI limit the outage probability to approximately 10^{-2} at high SNRs (20 dB), especially when using a small number of RIS elements ($N = 4$). This combined distortion, with SI alone causing an outage floor around 8×10^{-3}, poses a significant challenge in FD, resulting in HD systems outperforming FD across all SNR levels. Increasing the number of RIS elements (from N=4 to N=8) enhances FD performance, particularly in the presence of HIs, but does not eliminate the error floor. Thus, while RIS improves reliability, both SI and HIs inherently limit FD system performance, necessitating more RIS elements for competitive results.

Fig. 4 shows outage probabilities for RIS-FD/HD-HIs/IHIs versus N. The analytical results are presented for 0 dB and -10 dB SNR, $\Re = 4$ BPCU, $k^2_{S_1S_2} = 0.03$, and $\ell^2_{S_n} = 0.5$. The results indicate that increasing N in RIS effectively reduces the impact of both HIs and SI. Specifically, at an SNR of 0 dB, the proposed RIS-assisted bi-directional FD with HIs system significantly reduces the outage probability from 10^0 to 10^{-4} as N increases from 3 to 18. Accordingly, the

TABLE IV
OUTAGE PERFORMANCE COMPARISON OF THE PROPOSED RIS-FD-HIS WITH BENCHMARK METHODS FOR DIFFERENT N

SNR (dB)	*Reflective Elements N*	*Proposed RIS-FD-HIs*	*RIS-FD-HIs*	*RIS-HD-HIs*	*RIS-HD-IHIs*
-10 dB	3	1	1	1	1
	10	0.75	0.7	0.6	0.55
	20	0.55	0.5	0.35	0.3
	30	0.45	0.4	0.25	0.2
0 dB	3	1	1	1	1
	10	0.4	0.3	0.15	0.1
	18	10^{-4}	10^{-5}	10^{-3}	10^{-4}
	30	10^{-3}	5×10^{-4}	10^{-4}	5×10^{-5}

outage probabilities of the RIS-FD-IHIs and RIS-HD-HIs/IHIs systems indicate a similar decreasing trend with increasing N. However, at -10 dB SNR, the outage probabilities for both the RIS-FD/HD-HI systems are nearly the same owing to reduced SI. Similarly, the outage probabilities of the RIS-FD/HD-IHIs systems are comparable. Therefore, at a low transmit SNR of -10 dB, the impact of HIs is more dominant than SI in influencing the RIS aided systems performance. Moreover, it can be observed from the outage performance comparison Table IV that increasing N from 3 to 50 significantly lowers outage probability, showing RIS benefit to reliability. RIS-FD-HIs has high outage at low N, but improves beyond $N \approx 18$ (0 dB), dropping from 1 to 10^-4. HD systems have lower outage across all N and SNR. Therefore, larger RIS mitigates HIs/SI issues.

Fig. 5 presents a comparison of throughput performance for the proposed RIS-FD-HIs system in relation to RIS-FD-IHIs, RIS-HD-HIs, and RIS-HD-IHIs, with parameters set at $k^2_{S_1S_2} = 0.01$, $N = 4$, $m = 1$, $\Omega = 1$, and $\ell^2_{S_n} = 0.5$. Based on (29), analytical results for different configurations of RIS aided systems throughput are plotted. Although FD technology has the potential to double the data rates when compared to HD systems, it is noteworthy that the throughput of the proposed RIS-FD-HIs system is observed to be only half that of the RIS-HD-HIs/IHIs systems. This is attributed

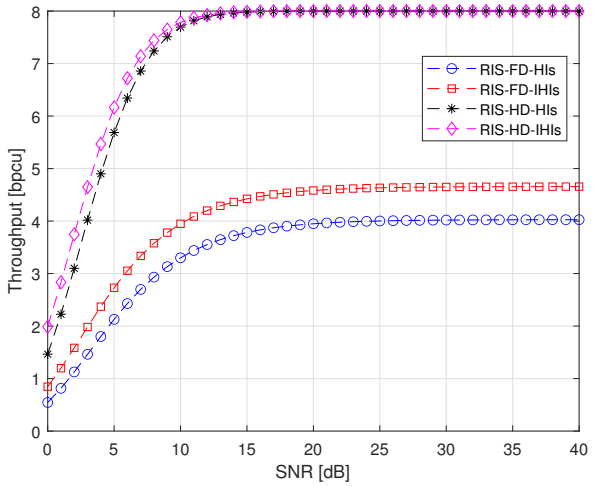

Fig. 5. Throughput comparison of the proposed RIS-FD-HIs system against RIS-FD-IHIs, RIS-HD-HIs, and RIS-HD-IHIs.

to the effects of both HIs and SI. For instance, at an SNR of 20 dB, the RIS-HD-HIs and RIS-HD-IHIs systems achieve a throughput of 8 BPCU, whereas the proposed RIS-assisted FD with and without HIs (RIS-FD-HIs & RIS-FD-IHIs) systems attain only 4 BPCU. This difference is due to the combined effects of HIs and SI. Therefore, it is crucial to implement effective strategies for mitigating both SI and HIs to enhance the overall performance of the system.

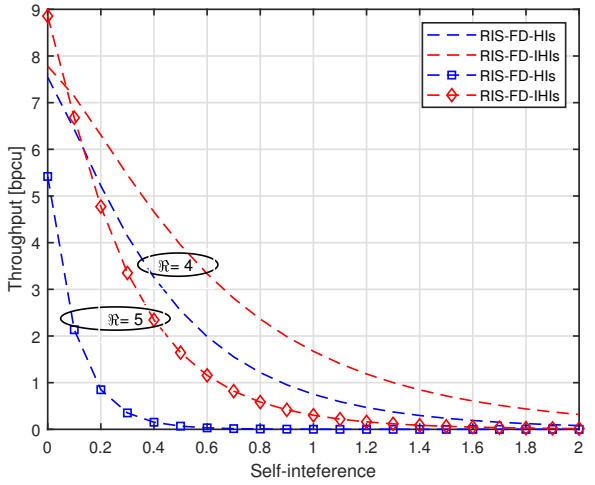

Fig. 6. System throughput versus self-interference $\ell^2_{S_n}$ at $\Re = 4$ and 5.

Fig. 6 presents the throughput performance analysis of the proposed RIS-assisted bi-directional FD systems, considering SI $\ell^2_{S_n}$, with and without HIs. The results are shown for fixed parameters of $\Re = 4$, and 5, $k^2_{S_1S_2} = 0.02$, and $N = 4$, respectively. The results indicate that an increase in $\ell^2_{S_n}$ from 0 to 0.2, leads to a substantial reduction in the proposed system's throughput. Specifically, for $\Re = 5$, the throughput decreases from approximately 5.5 to 1 BPCU. Similarly, when $\Re = 4$, the throughput declines from approximately 7.5 to approximately 5 BPCU. Therefore, it is evident that a notable

TABLE V
COMPARISON OF THROUGHPUT AND ENERGY EFFICIENCY OF THE PROPOSED RIS-FD-HIS WORK WITH BENCHMARK METHODS.

Performance Metric	*Parameter*	*Proposed RIS-FD-HIs*	*RIS-FD-IHIs*	*RIS-HD-HIs*	*RIS-HD-IHIs*
Throughput	SNR=20 dB, $N = 4$	4	4.5	8	8
Energy Efficiency	SNR=12 dB, $N = 2$	8.8	10.8	27.8	29.6
	SNR=4 dB $N = 6$	26	28	31.2	32

increase in the SI leads to a considerable reduction in the system throughput.

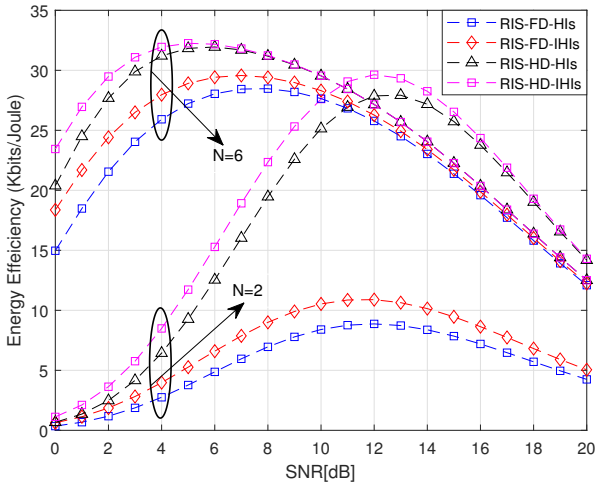

Fig. 7. Energy efficiency of the proposed RIS-FD-HIs systems as a function of SNR.

A. Design Guidelines for RIS-FD-HIs

The findings provide design guidelines for the implementation of RIS-FD-HIs under Nakagami-m channel fading environment.

- To limit the outage probability below 10^{-3} under HIs $k^2_{S_1S_2} = 0.01$, $\ell^2_{S_n} = 0.1$: Use $N > 8$ Fig. (2, 3).
- For throughput > 4 BPCU at 20 dB SNR: Use $N \geq 16$ or reduce $\ell^2_{S_n} < 0.05$ Fig. (5, 6).
- To maintain 90% of ideal throughput, $\ell^2_{S_n}$ must be less than 0.05, requiring analog and digital cancellation.
- For energy efficiency: Use lower value of reflective elements $N = 2$ at high SNR (> 12 dB); large $N = 6$ at low SNR (< 4dB) Fig. 7.
- Saturation loss can be limited to less than 2 dB when $k^2_{S_1S_2} < 0.01$; however, exceeding 0.03 results in irreducible error floors, even at N=64.

These guidelines harmonize linear power scaling (31) with impairment mitigation, thereby facilitating the effective deployment of RIS-FD.

Fig. 7 presents the energy efficiency analysis as a function of the SNR of the proposed RIS-assisted bi-directional FD systems. The simulation parameters are configured as follows:$\Re = 4$ BPCU, $N = 2$ and 6, $k^2_{S_1S_2} = 0.01$, $\bar{P}_l = 6$ dBm, $\ell^2_{S_n} = 0.2$, and $\bar{P}_{S_n}, n = 1, 2 = 10$ dBm, respectively. Based on (31) and the specified parameters, the analysis highlights the effect of varying N on achieving optimal energy

efficiency in RIS-assisted FD systems, even in the presence of hardware impairment. The findings suggest that the maximum energy efficiency η is achieved by reducing N when the transmit SNR is high. Conversely, increasing N enhances the energy efficiency in scenarios with lower transmit SNR values. For example, when the SNR is around 12 dB with $N = 2$, the maximum energy efficiencies are $8.8, 10.8, 27.8$, and 29.6 Kbit/joule are achieved for RIS-FD-HIs, RIS-FD-IHIs, RIS-HD-HIs, and RIS-HD-IHIs, respectively. Furthermore, with $N = 6$ and an SNR of 4 dB, these efficiencies reach values of $26, 28, 31.2$, and 32 Kbits/joule. In addition, Table V presents a comparative analysis of the proposed work's throughput and energy efficiency against benchmark systems. Although FD technology promises doubled spectral efficiency, HIs and SI in RIS-assisted FD systems often diminish throughput to levels comparable to HD systems. However, throughput of FD is highly susceptible to SI, effective suppression is crucial. Furthermore, FD systems typically exhibit lower energy efficiency than HD systems due to HIs and SI. While increasing N enhances energy efficiency at low SNRs, a smaller N proves more efficient at high SNRs. Therefore, these findings suggest that increasing N effectively enhances the performance of the proposed RIS-assisted bi-directional FD systems.

VI. Conclusion

This paper investigated the performance of RIS-assisted FD systems by considering the effects of both HIs and SI under Nakagami-m fading. Analytical expressions were derived initially for the SINDR and channel coefficient distributions. These expressions are then used to formulate the performance metrics, including the outage probability, asymptotic outage probability, system throughput, and energy efficiency. The RIS-FD design guidelines, accounting for potential impairments strengthens the practical value. The numerical results indicate that the HIs and SI significantly affect the system performance. Furthermore, it has been observed that the non-ideal parameters of RIS-FD systems result in an error floor at higher values of SNR, particularly when N is small, thereby degrading the outage probability. Increasing N and implementing effective deployment strategies can mitigate the combined effects of HIs and SI. The proposed RIS-FD system incorporating HIs exhibits enhanced outage probability, throughput, and energy efficiency compared to RIS-FD, RIS-HD systems with and without HIs, especially when the RIS is equipped with a sufficient number of reflective elements. Furthermore, a comprehensive analysis analyzes the impact of key performance parameters, such as the number of reflecting elements, SI levels, and hardware impairment severity, on overall system performance.

References

[1] Z. Zhang, Y. Xiao, Z. Ma, M. Xiao, Z. Ding, X. Lei, G. K. Karagiannidis, and P. Fan, "6G wireless networks: Vision, requirements, architecture, and key technologies," *IEEE Vehicular Technology Magazine*, vol. 14, no. 3, pp. 28–41, 2019.

[2] C.-X. Wang, J. Huang, H. Wang, X. Gao, X. You, and Y. Hao, "6G wireless channel measurements and models: Trends and challenges," *IEEE Vehicular Technology Magazine*, vol. 15, no. 4, pp. 22–32, 2020.

[3] W. Zhang, Z. Wen, C. Du, Y. Jiang, and B. Zhou, "RIS-assisted self-interference mitigation for in-band FD transceivers," *IEEE Transactions on Communications*, vol. 71, no. 9, pp. 5444–5454, 2023.

[4] A. Salem, K.-K. Wong, C.-B. Chae, and Y. Zhang, "STAR-RIS-assisted FD NOMA communication networks," *IEEE Transactions on Wireless Communications*, vol. 24, no. 3, pp. 2467–2482, 2025.

[5] G. C. Alexandropoulos, M. A. Islam, and B. Smida, "FD massive MIMO architectures: Recent advances, applications, and future directions," *arXiv preprint arXiv:2205.08393*, 2022.

[6] N. Shlezinger, G. C. Alexandropoulos, M. F. Imani, Y. C. Eldar, and D. R. Smith, "Dynamic metasurface antennas for 6G extreme massive MIMO communications," *IEEE Wireless Communications*, vol. 28, no. 2, pp. 106–113, 2021.

[7] A. Papazafeiropoulos, P. Kourtessis, S. Chatzinotas, D. I. Kaklamani, and I. S. Venieris, "STARS-enabled full-duplex two-way mMIMO system under spatially correlated channels," *IEEE Transactions on Vehicular Technology*, vol. 74, no. 7, pp. 10 495–10 509, 2025.

[8] K. M. S. Huq, S. A. Busari, J. Rodriguez, V. Frascolla, W. Bazzi, and D. C. Sicker, "Terahertz-enabled wireless systems for beyond-5G ultra-fast networks: A brief survey," *IEEE Network*, vol. 33, no. 4, pp. 89–95, 2019.

[9] P. Mach and Z. Becvar, "Device-to-device relaying: Optimization, performance perspectives, and open challenges toward 6G networks," *IEEE Communications Surveys & Tutorials*, vol. 24, no. 3, pp. 1336–1393, 2022.

[10] S. P. Dash and A. Kaushik, "RIS-assisted 6G wireless communications: A novel statistical framework in the presence of direct channel," *IEEE Communications Letters*, vol. 28, no. 3, pp. 717–721, 2024.

[11] B. Smida, A. Sabharwal, G. Fodor, G. C. Alexandropoulos, H. A. Suraweera, and C.-B. Chae, "FD wireless for 6G: Progress brings new opportunities and challenges," *IEEE Journal on Selected Areas in Communications*, vol. 41, no. 9, pp. 2729–2750, 2023.

[12] K. Shafique and M. Alhassoun, "Going beyond a simple RIS: Trends and techniques paving the path of future RIS," *IEEE Open Journal of Antennas and Propagation*, vol. 5, no. 2, pp. 256–276, 2024.

[13] Y. Wang, W. Zhang, Y. Chen, C.-X. Wang, and J. Sun, "Novel multiple RIS-assisted communications for 6G networks," *IEEE Communications Letters*, vol. 26, no. 6, pp. 1413–1417, 2022.

[14] Z. Cui, K. Guan, J. Zhang, and Z. Zhong, "SNR coverage probability analysis of RIS-aided communication systems," *IEEE Transactions on Vehicular Technology*, vol. 70, no. 4, pp. 3914–3919, 2021.

[15] E. Björnson and L. Sanguinetti, "Rayleigh fading modeling and channel hardening for reconfigurable intelligent surfaces," *IEEE Wireless Communications Letters*, vol. 10, no. 4, pp. 830–834, 2021.

[16] D. T. Tam, B. C. Nguyen, N. V. Vinh *et al.*, "Outage and throughput performance of hybrid RIS–relay-aided wireless systems with imperfect transceiver hardware," *AEU – International Journal of Electronics and Communications*, vol. 157, p. 154425, 2022.

[17] W. Khalid, H. Yu, J. Cho, Z. Kaleem, and S. Ahmad, "Rate–energy tradeoff analysis in RIS-SWIPT systems with hardware impairments and phase-based amplitude response," *IEEE Access*, vol. 10, pp. 31 821–31 835, 2022.

[18] Y. Xu, H. Xie, Q. Wu, C. Huang, and C. Yuen, "Robust max–min energy efficiency for RIS-aided HetNets with distortion noises," *IEEE Transactions on Communications*, vol. 70, no. 2, pp. 1457–1471, 2022.

[19] K. Guo and K. An, "On the performance of RIS-assisted integrated satellite–UAV–terrestrial networks with hardware impairments and interference," *IEEE Wireless Communications Letters*, vol. 11, no. 1, pp. 131–135, 2022.

[20] J. Dai, F. Zhu, C. Pan, H. Ren, and K. Wang, "Statistical CSI-based transmission design for RIS-aided massive MIMO systems with hardware impairments," *IEEE Wireless Communications Letters*, vol. 11, no. 1, pp. 38–42, 2022.

[21] M. H. N. Shaikh, V. A. Bohara, A. Srivastava, and G. Ghatak, "Performance analysis of intelligent reflecting surface-assisted wireless systems with non-ideal transceivers," *IEEE Open Journal of the Communications Society*, vol. 2, pp. 671–686, 2021.

[22] A.-A. A. Boulogeorgos and A. Alexiou, "How much do hardware imperfections affect the performance of reconfigurable intelligent surface-assisted systems?" *IEEE Open Journal of the Communications Society*, vol. 1, pp. 1185–1195, 2020.

[23] S. Zhou, W. Xu, K. Wang, M. D. Renzo, and M.-S. Alouini, "Spectral and energy efficiency of IRS-assisted MISO communication with hardware impairments," *IEEE Wireless Communications Letters*, vol. 9, no. 9, pp. 1366–1369, 2020.

[24] Y. Zhang, W. Xia, H. Zhao, G. Zheng, S. Lambotharan, and L. Yang, "Performance analysis of RIS-assisted cell-free massive MIMO systems

with transceiver hardware impairments," *IEEE Transactions on Communications*, vol. 71, no. 12, pp. 7258–7272, 2023.

[25] Q. Li, M. El-Hajjar, Y. Sun, I. Hemadeh, A. Shojaeifard, Y. Liu, and L. Hanzo, "Achievable rate analysis of the STAR-RIS-aided NOMA uplink with imperfect CSI and hardware impairments," *IEEE Transactions on Communications*, vol. 71, no. 10, pp. 6100–6114, 2023.

[26] I. Yildirim, F. Kilinc, E. Basar, and G. C. Alexandropoulos, "Hybrid RIS-empowered reflection and decode-and-forward relaying for coverage extension," *IEEE Communications Letters*, vol. 25, no. 5, pp. 1692–1696, 2021.

[27] Z. Abdullah, G. C. Alexandropoulos, S. Kisseleff, S. Chatzinotas, and B. Ottersten, "Combining relaying and reflective surfaces: Power consumption and energy efficiency analysis," in *Proc. IEEE GLOBECOM Workshops*, 2022, pp. 31–36.

[28] S. Atapattu, R. Fan, P. Dharmawansa, G. Wang, J. Evans, and T. A. Tsiftsis, "Reconfigurable intelligent surface-assisted two-way communications: Performance analysis and optimization," *IEEE Transactions on Communications*, vol. 68, no. 10, pp. 6552–6567, 2020.

[29] Z. Peng, Z. Zhang, C. Pan, L. Li, and A. L. Swindlehurst, "Multiuser FD two-way communications via intelligent reflecting surface," *IEEE Transactions on Signal Processing*, vol. 69, pp. 837–851, 2021.

[30] J. Wang, Y.-C. Liang, J. Joung, X. Yuan, and X. Wang, "Joint beamforming and RIS design for two-way relay networks," *IEEE Transactions on Communications*, vol. 69, no. 8, pp. 5620–5633, 2021.

[31] Z. Liu, X. Yue, C. Zhang, Y. Liu, Y. Yao, Y. Wang, and Z. Ding, "Performance analysis of RIS-assisted two-way NOMA networks," *IEEE Transactions on Vehicular Technology*, vol. 71, no. 12, pp. 13 091–13 104, 2022.

[32] B. C. Nguyen, T. M. Hoang, T. Kim *et al.*, "On the performance of two-way full-duplex communication systems with reconfigurable intelligent surfaces," *IEEE Access*, vol. 9, pp. 81 274–81 285, 2021.

[33] Y. Tao, Q. Li, and X. Ge, "Sum-rate optimization for IRS-aided two-way AF relay systems," in *Proc. IEEE/CIC Int. Conf. on Communications in China (ICCC)*, 2021, pp. 823–828.

[34] T. H. Nguyen and T. T. Nguyen, "On performance of STAR-RIS-enabled multiple two-way FD D2D communication systems," *IEEE Access*, vol. 10, pp. 89 063–89 071, 2022.

[35] P. Zhang, X. Wang, S. Feng, Z. Sun, F. Shu, and J. Wang, "Phase optimization for massive IRS-aided two-way relay network," *IEEE Open Journal of the Communications Society*, vol. 3, pp. 1025–1034, 2022.

[36] C. N. Efrem and I. Krikidis, "IRS deployment optimization in multi-IRS-assisted two-way FD communication systems," in *Proc. IEEE Int. Conf. on Communications (ICC)*, 2022, pp. 4685–4690.

[37] B. Lu, R. Wang, and Y. Liu, "Outage probability of intelligent reflecting surface-assisted FD two-way communications," *IEEE Communications Letters*, vol. 26, no. 2, pp. 286–290, 2022.

[38] P. Saikia, S. Pala, K. Singh, S. K. Singh, and W.-J. Huang, "Proximal policy optimization for RIS-assisted full-duplex 6G-V2X communications," *IEEE Transactions on Intelligent Vehicles*, vol. 9, no. 7, pp. 5134–5149, 2024.

[39] Q. Li, D. Xu, K. Zhang, K. Navaie, and Z. Ding, "Covert communications in STAR-RIS-assisted NOMA IoT networks over Nakagami-m fading channels," *IEEE Internet of Things Journal*, vol. 11, no. 12, pp. 22 456–22 470, 2024.

[40] S. Yadav, A. K. Yadav, R. Gour, G. C. Alexandropoulos, and D. S. Gurjar, "Two-way communications empowered by reconfigurable intelligent surfaces and direct link: Outage analysis under hardware impairments and Nakagami-m fading," *Physical Communication*, vol. 64, p. 102352, 2024.

[41] D. Kumar, P. K. Singya, O. Krejcar, K. Choi, and V. Bhatia, "Performance of IRS-aided FD two-way communication networks with imperfect SIC," *IEEE Transactions on Vehicular Technology*, vol. 72, no. 4, pp. 5491–5496, 2023.

[42] T.-H. Vu and S. Kim, "Performance analysis of FD two-way RIS-based systems with imperfect CSI and discrete phase-shift design," *IEEE Communications Letters*, vol. 27, no. 2, pp. 512–516, 2023.

[43] T. N. Nguyen, N. N. Thang, B. C. Nguyen, T. M. Hoang, and P. T. Tran, "Intelligent reflecting surface-aided bidirectional FD communication systems with imperfect self-interference cancellation and hardware impairments," *IEEE Systems Journal*, vol. 17, no. 1, pp. 1352–1362, 2023.

[44] G. Kumar Pandey, D. Singh Gurjar, S. Yadav, D. Krstic, and Y. Jiang, "Secrecy analysis and optimization of uav-assisted iot networks with rf-eh and imperfect hardware," *IEEE Internet of Things Journal*, vol. 12, no. 7, pp. 8049–8063, 2025.

[45] G. K. Pandey, D. S. Gurjar, S. Yadav, R. Hazra, and X. Li, "Drl-driven star-ris assisted secure communication with hppp eavesdroppers," *IEEE Communications Letters*, vol. 30, pp. 352–356, 2026.

[46] C. K. Sheemar, G. C. Alexandropoulos, D. Slock, J. Querol, and S. Chatzinotas, "FD-enabled joint communications and sensing with reconfigurable intelligent surfaces," in *Proc. European Signal Processing Conf. (EUSIPCO)*, 2023, pp. 1509–1513.

[47] T. Wang, G. Chen, and J. P. Coon, "Performance analysis of RIS-assisted FD communication over correlated Nakagami-m fading channels," *IEEE Transactions on Vehicular Technology*, vol. 73, no. 3, pp. 3430–3444, 2023.

[48] T. N. Nguyen, N. V. Vinh, B. C. Nguyen, and B. V. Minh, "On the performance of RIS-aided bidirectional full-duplex systems with combining of imperfect conditions," *Wireless Networks*, vol. 30, no. 2, pp. 649–660, 2024.

[49] A.-A. A. Boulogeorgos, E. N. Papasotiriou, and A. Alexiou, "Analytical performance assessment of THz wireless systems," *IEEE Access*, vol. 7, pp. 11 436–11 453, 2019.

[50] A. Sabharwal, P. Schniter, D. Guo, D. W. Bliss, S. Rangarajan, and R. Wichman, "In-band full-duplex wireless: Challenges and opportunities," *IEEE Journal on selected areas in communications*, vol. 32, no. 9, pp. 1637–1652, 2014.

[51] I. S. Gradshteyn and I. M. Ryzhik, *Table of Integrals, Series, and Products*. Academic Press, 2014.

[52] S. Li, S. Yan, L. Bariah, S. Muhaidat, and A. Wang, "IRS-assisted full-duplex systems over rician and Nakagami-m fading channels," *IEEE Open Journal of Vehicular Technology*, vol. 4, pp. 217–229, 2023.

[53] S. Primak, V. Kontorovich, and V. Lyandres, *Stochastic Methods and Their Applications to Communications: Stochastic Differential Equations Approach*. John Wiley & Sons, 2005.

[54] J. G. Proakis and M. Salehi, *Digital communications*. McGraw-hill, 2008.

[55] M. H. Samuh, A. M. Salhab, and A. H. A. El-Malek, "Performance analysis and optimization of RIS-assisted networks in Nakagami-m environment," *arXiv preprint arXiv:2010.07841*, 2020.

[56] L. B. Kumar, R. P. Naik, P. Krishnan, A. A. B. Raj, A. K. Majumdar, and W.-Y. Chung, "RIS-assisted triple-hop RF–FSO convergent with UWOC system," *IEEE Access*, vol. 10, pp. 66 564–66 575, 2022.

[57] S. R. Kudumala, A. K. Dubey, P. Gupta, S. Gupta, and E. Sharma, "Hardware-impaired RIS-assisted multi-pair FD communication with spatial correlation," *IEEE Communications Letters*, vol. 26, no. 9, pp. 2200–2204, 2022.

[58] J. Choi, "Joint rate and power allocation for NOMA with statistical CSI," *IEEE Transactions on Communications*, vol. 65, no. 10, pp. 4519–4528, 2017.

R. Ramanathan received the B.E. degree in Electronics and Communication engineering from Mohammad Sathak college of Engineering, Kilakarai, India in 2002, M.Tech. degree in Communication Engineering 2005, and the Ph.D. degree from Vellore Institute of Technology (VIT), vellore, in 2019. He is now an Associate professor in the School of Electronics Engineering, VIT, Vellore. His research interest includes signal processing in FD relay assisted communication, reflective intelligent surface systems, and multi-input-multi-output wireless communication.

A. Bagubali received the Bachelor of Technology (B.Tech.) degree in electronics and communication engineering, and the Master of Technology (M.Tech.) and Doctor of Philosophy (Ph.D.) degrees in communication engineering from Vellore Institute of Technology (VIT), Vellore, Tamil Nadu, in 2005, April 2007, and June 2019, respectively. He is currently an Associate Professor with the School of Electronics Engineering (SENSE), VIT. He has published more than 20 articles in national and international journals. His research interests include IP multimedia subsystems in 3G and 4G networks and wireless and wireless sensor networks.